

# Benchmark of the FLUKA model of crystal channeling against the UA9-H8 experiment



P. Schoofs<sup>a,\*</sup>, F. Cerutti<sup>a</sup>, A. Ferrari<sup>a</sup>, G. Smirnov<sup>a,b</sup>

<sup>a</sup>European Organization for Nuclear Research (CERN), Geneva, Switzerland

<sup>b</sup>Joint Institute for Nuclear Research (JINR), Dubna, Russia

## ARTICLE INFO

### Article history:

Received 29 November 2014

Received in revised form 18 March 2015

Accepted 18 March 2015

Available online 24 April 2015

### Keywords:

Crystal channeling

Monte Carlo

FLUKA

Benchmark

UA9 collaboration

## ABSTRACT

Channeling in bent crystals is increasingly considered as an option for the collimation of high-energy particle beams. The installation of crystals in the LHC has taken place during this past year and aims at demonstrating the feasibility of crystal collimation and a possible cleaning efficiency improvement. The performance of CERN collimation insertions is evaluated with the Monte Carlo code FLUKA, which is capable to simulate energy deposition in collimators as well as beam loss monitor signals. A new model of crystal channeling was developed specifically so that similar simulations can be conducted in the case of crystal-assisted collimation. In this paper, most recent results of this model are brought forward in the framework of a joint activity inside the UA9 collaboration to benchmark the different simulation tools available. The performance of crystal STF 45, produced at INFN Ferrara, was measured at the H8 beamline at CERN in 2010 and serves as the basis to the comparison. Distributions of deflected particles are shown to be in very good agreement with experimental data. Calculated dechanneling lengths and crystal performance in the transition region between amorphous regime and volume reflection are also close to the measured ones.

© 2015 CERN for the benefit of the Authors. Published by Elsevier B.V. This is an open access article under the CC BY license (<http://creativecommons.org/licenses/by/4.0/>).

## 1. Introduction

Crystals are increasingly used in synchrotrons around the world for their channeling properties. At CERN, two technologies of crystals will be used to conduct an experiment at the LHC [1,2]. The efficiency of a strip and a quasi-mosaic crystal deflector is planned to be measured in a low-intensity beam close to the nominal energy [3]. This novel experimental activity aims at investigating the use of crystal collimation as an upgrade option for the current system, which performed very well during the past LHC run and will be confronted with more demanding conditions in the coming years. Crystal collimation consists in the use of a bent crystal as particle deflector instead of a primary amorphous collimator (60 cm of carbon composite in the LHC), deflecting part of the beam halo onto a secondary absorber. The density of particles impacting on the absorber is expected to be higher than in the current system, and the absorber has to be specifically designed to withstand this increased load. On the other hand, crystal collimation is expected to be advantageous in reducing losses in critical parts of the machine (such as the dispersion suppressor) coming mainly from single-diffractive events, which are strongly reduced through the use of short crystals compared to a massive collimator jaw [4].

At CERN, the Monte Carlo code FLUKA is used to perform beam-machine interaction studies [5,6]. It is used to calculate the particle shower originated in the current collimation system and, in view of the possible insertion of crystals as an ingredient of the future collimation system, a complementing module has been designed to be able to deal with coherent effects taking such as channeling, volume reflection and volume capture. For the moment this model is limited to planar channeling of positively charged particles as applications at CERN are the focus of the work.

The event generator, described at length in [7], relies on a semi-classical approach. The Moliere potential is altered by the atomic thermal motion and, in the case of a bent crystal, by a centrifugal term weakening the potential confinement. Inside the crystal, particles undergo single Coulomb and nuclear scattering possibly leading to dechanneling. These events are however less frequent than in a so-called amorphous orientation, where no coherent effect is taking place, because of the increased mean distance between the particle and the atomic nuclei along its trajectory.

## 2. Framework of the study

The UA9 collaboration is studying the feasibility and performance of a crystal-assisted collimation system at CERN. As part of its activity, several simulation codes are under development

\* Corresponding author.

which are helping to predict efficiency and degradation of the crystal in unprecedented energy and intensity conditions. The benchmarking conducted in this paper is part of a joint effort by the code developers to provide a clear perspective on the different strengths of the tools available for use in the collaboration. The measurements considered as basis for this common benchmarking are the ones performed on a 400 GeV/c proton beam in the years 2010–2012 at CERN H8 beamline. The critical channeling angle at this energy is close to  $10\ \mu\text{rad}$ , comparable to the beam divergence. Data from this experiment has been extensively analyzed and parameters and results have been made available by Rossi [8]. The joint effort has in particular focused on crystal STF45 from Ferrara [1,9], a 2-mm long silicon strip with a bending angle of  $143.8\ \mu\text{rad}$  (which corresponds to a bending radius of 13.91 m).

The experimental setup consists of 5 silicon tracker planes that are situated around the crystal. Two planes are placed upstream of the crystal and three ownstream. The telescope is reconstructing both arms of the particle trajectory leading to a corresponding hit position and deflection angle at the crystal location.

Data from the experiment is corrected for crystal torsion (causing a shift in orientation along the crystal longest dimension). Even though the FLUKA model of crystal channeling can handle a constant crystal torsion, the decision was to compensate for it at data analysis level, not to discriminate codes on their capability to reproduce it.

The crystal was maintained in a constant channeling orientation throughout the experiment. However, the divergence of the beam was  $10.65\ \mu\text{rad}$  in the horizontal plane and  $7.68\ \mu\text{rad}$  in the vertical one, which means that some particles are coming onto the crystal with an angle larger than the critical angle. This allows to perform analysis not only in channeling but also in volume reflection.

The detector resolution has to be taken into account, in the experimental results. It has been estimated in [10] and equals  $2.8\ \mu\text{rad}$  for the upstream arm of the telescope and  $5.2\ \mu\text{rad}$  for the whole tracking system. To better appreciate the comparison between simulation and experiment, this uncertainty has been added accordingly in the simulation. Contribution to multiple Coulomb scattering from the detectors is also taken into account in the simulation.

It should be noted that the crystal was positioned in a way that the coherent deflection given by the (110) planar channels is purely horizontal and the following results are focused on the horizontal dimension.

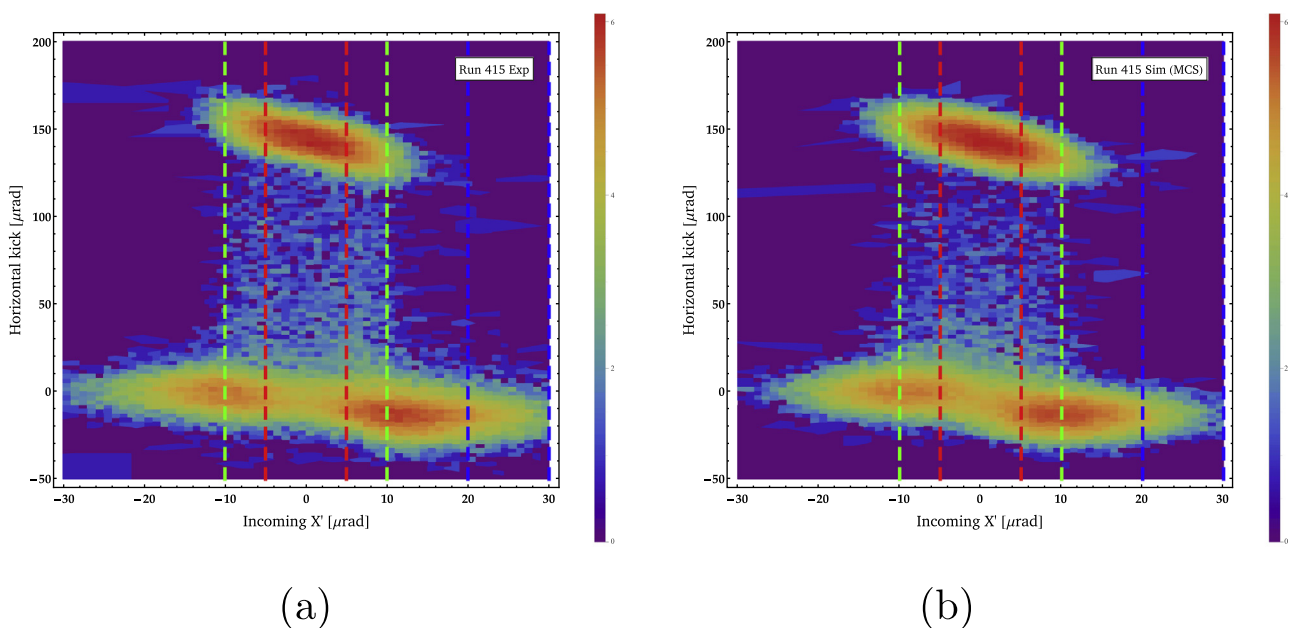
### 3. Results

#### 3.1. Channeling

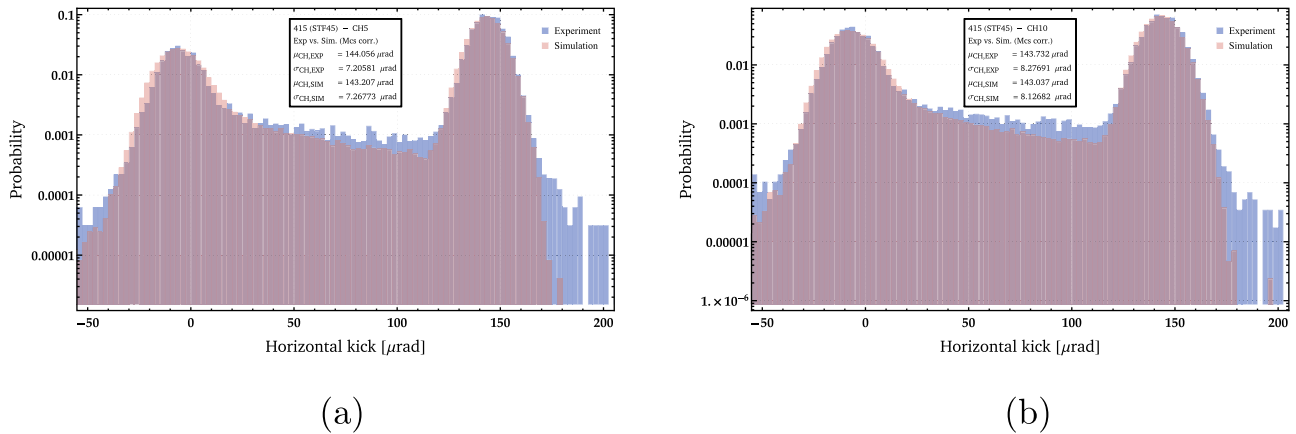
Fig. 1 shows the 2D-distribution of particles as a function of the (horizontal) incoming angle and the deflection imparted by the crystal. Fig. 1(a) refers to the experiment, while Fig. 1(b) refers to the simulation. This figure shows the similarities between calculations and measurements for the different orientations. From the left to the right of the figure, the distribution shows the amorphous behavior followed by the channeling region, then the volume reflection one. This figure shows as well that transitions between the different modes are well simulated by the FLUKA module. In the following, deflections distributions are analyzed for specific orientations, denoted by dashed lines.

Fig. 2 shows the deflection distributions in the two channeling windows: (a) within  $5\ \mu\text{rad}$  and (b)  $10\ \mu\text{rad}$  of the channel orientation. The left-hand side peak is comprised of particles that do not enter channeling, some of them being reflected, and the others crossing the crystal as they would an amorphous device. This double peak is non-Gaussian and the estimation of its standard deviation is about 5% higher than it is for the experiment. Although this difference is small, it indicates that the volume reflection angle is in this case, slightly overestimated by the geometrical model, pulling the two components of the peak apart. The right-hand side peak is formed by particles channeled from the beginning of the crystal to its end-face. In between are dechanneled particles, distributed exponentially as is visible on the graphs. The dechanneling length can be estimated with a fit of the distribution in between the two peaks. Fig. 3 shows such a fit, and the corresponding value of the dechanneling length, for the simulation of the narrow window case. Values of the mean and standard deviation of the peaks as well as dechanneling length are summarized in Table 1.

The channeling rate is the fraction of particles belonging to the channeling peak ( $\pm 3\sigma$ ). The dechanneling rate is the fraction of



**Fig. 1.** Particle distribution as (a) measured (b) simulated as a function of the particle incoming angle ( $x$ -axis) and of the horizontal deflection imparted by the crystal ( $y$ -axis). Dashed lines indicate regions of interest treated in the analysis. Green: within  $10\ \mu\text{rad}$  of the channel orientation. Red: within  $5\ \mu\text{rad}$ . Blue: in the volume reflection region. (For interpretation of the references to color in this figure legend, the reader is referred to the web version of this article.)



**Fig. 2.** Measured and simulated deflection distributions of 400 GeV-protons in crystal STF 45. (a) Only particles incoming within 5  $\mu\text{rad}$  of the channel orientation are considered. (b) Only particles incoming within 10  $\mu\text{rad}$  are considered.

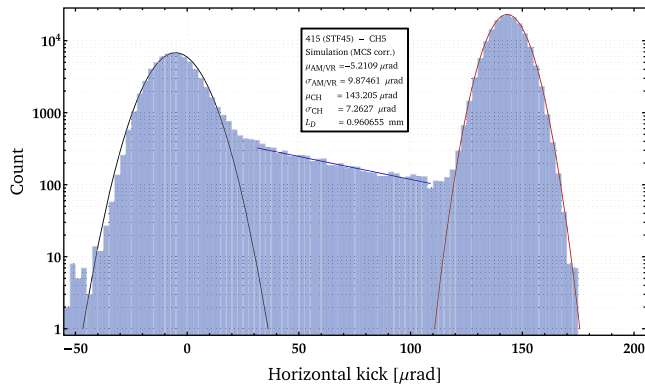


**Fig. 3.** Simulated deflection distribution in the case of a narrow 5  $\mu\text{rad}$  filter in the incoming angle. The dechanneling length is calculated through an exponential fit on the dechanneled particles distribution in between the peaks.

particles in between the two peaks (outside of  $3\sigma$ ). We can see in table 1 that the agreement is very good in terms of channeling rate. The dechanneling rate on the other hand is underestimated by about 25% and a dechanneling length discrepancy of 35–40% is observed. This means that particles have a tendency to be lost sooner in the crystal and the distribution of dechanneled particles is shifted to low angles. The suppression of Coulomb scattering in channeling regime by the means of a form factor [7] appears to be slightly underestimated. This is not to be confused with the dechanneling rate, which rather than a description of the dechanneling particles distribution, is a measure of the total amount of particles having dechanneled. In this case, we see less particles dechanneled in absolute and their average deflection is smaller

**Table 1**  
Mean and standard deviations of the volume reflected/non-channeled particles (VR/AM) and of the channeling peaks (CH) as well as dechanneling lengths for 400 GeV-protons in STF 45 strip crystal.

STF45	AM/VRpeak [ $\mu\text{rad}$ ]	CH peak [ $\mu\text{rad}$ ]	CH rate [%]	DC rate [%]	Dech. length [mm]
Cut at $\pm 5 \mu\text{rad}$					
Simulation	$-5.2 \sigma 9.9$	$143.2 \sigma 7.3$	$68.6 \pm 0.2$	$3.7 \pm 0.1$	$0.95 \pm 0.08$
Experiment	$-4.7 \sigma 9.2$	$144.1 \sigma 7.2$	$68.9 \pm 0.5$	$4.76 \pm 0.24$	1.42
Cut at $\pm 10 \mu\text{rad}$					
Simulation	$-6.3 \sigma 9.9$	$143.1 \sigma 8.1$	$56.8 \pm 0.2$	$3.7 \pm 0.1$	$0.95 \pm 0.08$
Experiment	$-5.9 \sigma 9.5$	$143.8 \sigma 8.0$	$54.0 \pm 0.4$	$5.13 \pm 0.18$	1.53

because of the smaller dechanneling length. This behaviour can vary depending on the form factor used to simulate the partial suppression of scattering for channeled particles. A rejection of the scattering process extended to larger impact parameters would lead to an increase of the dechanneling length, and at the same time to a reduction of the dechanneling rate (by a smaller relative amount).

### 3.2. Transition region

Some particles incoming at a small angle are not channeled. This so-called blocking regime is reproduced in the simulation by an increase of the potential transverse energy of the particle when it enters close to the crystal lattice plane (within a distance of the order of the Thomas–Fermi screening length), thus diminishing the probability of being channeled. The average deflection of those particles has been reported in Fig. 4(a) as a function of the incoming angle. In this figure, the deflection on the left, close to 0, corresponds to the average one of any amorphous material. On the right-hand side, the mean deflection stabilizes around the volume reflection angle. The experiment shows two unexpected slope variations that are not seen on other strip crystals of the same type and that we cannot yet explain. Fig. 4(b) shows an analogous plot for another strip crystal (STF 50) produced by the same method and the same institution, where the measured transition appears much smoother than in STF 45 and very close to the simulated one.

### 3.3. Volume reflection

In volume reflection orientation, incoming particles are not aligned well enough with the lattice to get channeled, but their trajectory is becoming parallel to the crystal planes as they progress in a bent crystal. Volume reflection results in a small kick in the

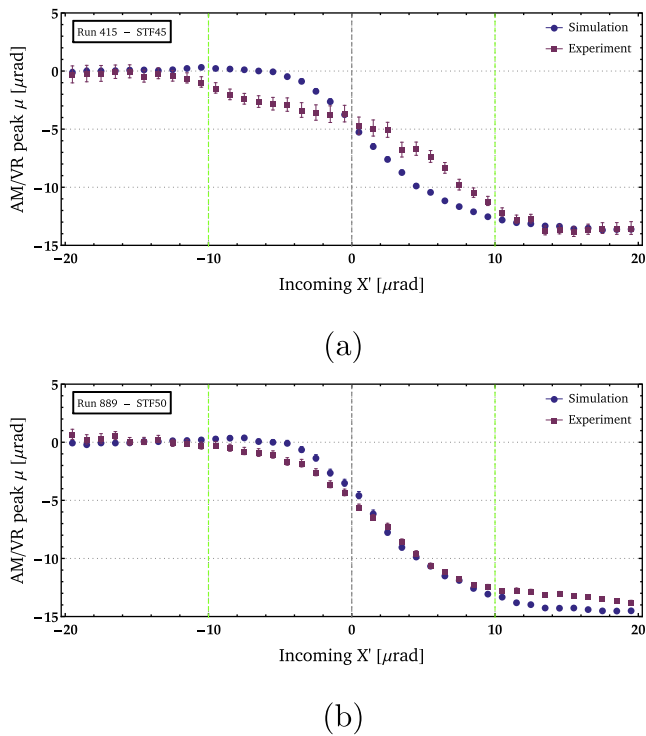


**Fig. 4.** Evolution of the average angular deflection given by the crystal to non-channeled particles as a function of the incoming angle. The transition region between the amorphous behavior of a non-oriented crystal (on the left) and the volume reflection region (on the right) is emphasized, (a) crystal STF 45 (b) crystal STF 50

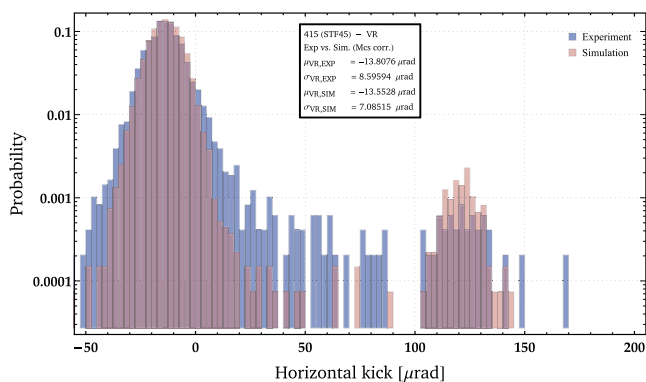


**Fig. 5.** Deflection distribution at the exit of the STF 45 crystal in volume reflection orientation (from 20 to 30  $\mu$ rad off the channel orientation).

direction opposite to the bend. This process is rival to the rarer one of volume capture in which the particle gets trapped in a channel inside the crystal after an interaction and continues its movement in channeling mode down the crystal. Fig. 5 shows the deflection distribution for particles incoming between 20  $\mu$ rad and 30  $\mu$ rad off the channel direction (positive angles, as the bend). There is a good match between the volume capture peaks, on the right-hand side, indicating a good volume capture rate as well. Subsequent dechanneling of captured particles is underestimated in the simulation, as the conditions of channeling after capture are not well understood yet and in the simulation no difference is made

between the channeling of a particle captured in the middle of the crystal with respect to a particle channeled since the beginning. The calculated and measured volume reflected peaks are very close to each other (left-hand side of the figure), confirming the accuracy of the geometrical model adopted for the description of by this mechanism.

#### 4. Conclusions

In this paper, we have presented the results of the benchmarking of the FLUKA model of crystal channeling in the specific case of crystal STF 45, chosen in conjunction with fellow code developers as a mean to standardize the benchmarks. Even though simulation codes are compared with a large number of runs available for analysis within the UA9 collaboration, only the aforementioned crystal has been presented here for the sake of conciseness and uniformity. The calculated deflection distribution for a 400-GeV proton beam is shown to be in good agreement with the experimental one. The channeling rate is well reproduced within a few percent and the peaks widths are within 10%. The simulated transition region has been shown to reproduce accurately strip crystal behaviour except in one case where the latter shows a peculiarity which is not fully understood. The dechanneling length is underestimated in the simulation by about 40%. This is leading as well to an underestimation of high-deflection dechanneled particles. On the other hand, the overall amount of dechanneled particles, indicated by the dechanneling rate, is about 25% below the experimental results. Additional studies are needed to determine how the dechanneling process description can be improved. Nevertheless the very good results obtained by this model in the reproduction of channeling efficiencies of crystals of different types [11] is encouraging, motivating further investigations at higher energies, up to 7 TeV.

#### References

- [1] S. Baricordi, V. Guidi, A. Mazzolari, G. Martinelli, A. Carnera, D. De Salvador, A. Sambo, G. Della Mea, R. Milan, A. Vomiero, W. Scandale, Optimal crystal surface for efficient channeling in the new generation of hadron machines, *Appl. Phys. Lett.* 91 (6) (2007) 061908. <<http://scitation.aip.org/content/aip/journal/apl/91/6/10.1063/1.2768200>>.
- [2] Y. Ivanov, A. Denisov, Y. Gavrikov, L. Lapina, L. Malyarenko, V. Skorobogatov, Quasi-Mosaic Silicon Crystal Deflectors for LHC Beams, 2014.
- [3] W. Scandale, et al., LHC Collimation with Bent Crystals – Letter of Intent, Tech. Rep. CERN-LHCC-2011-007, CERN, 2011.
- [4] D. Mirarchi, S. Montesano, W. Scandale, S. Redaelli, A. Taratin, F. Galluccio, Final layout and expected cleaning for the first crystal-assisted collimation test at the LHC, in: *Proceedings of IPAC 2014*, 2014.
- [5] A. Ferrari, P.R. Sala, A. Fasso, J. Ranft, FLUKA: A Multi-Particle Transport Code, Tech. Rep. CERN-2005-10, CERN, 2005.
- [6] G. Battistoni, S. Muraro, P.R. Sala et al., The FLUKA code: description and benchmarking, in: *Proceedings of the Hadronic Shower Simulation Workshop 2006*, HSS06, pp. 31–49.
- [7] P. Schoofs, F. Cerutti, A. Ferrari, G. Smirnov, Monte carlo modeling of crystal channeling at high energies, *Nucl. Instr. Meth. Phys. B* 309 (0) (2013) 115–119. <<http://www.sciencedirect.com/science/article/pii/S0168583X1300284X>>.
- [8] R. Rossi, D. Mirarchi, W. Scandale, G. Cavoto, S. Redaelli, measurements of coherent interactions in silicon bent crystals with 400 GeV-protons at CERN H8 (2014)\*\*
- [9] S. Baricordi, V. Guidi, A. Mazzolari, D. Vicenzi, M. Ferroni, Shaping of silicon crystals for channeling experiments through anisotropic chemical etching, *J. Phys. D* 41 (24) (2008) 245501. <<http://iopscience.iop.org/0022-3727/41/24/245501>>.
- [10] M. Pesaresi, W. Ferguson, J. Fulcher, G. Hall, M. Raymond, M. Ryan, O. Zorba, Design and performance of a high-rate, high angular resolution beam telescope used for crystal channeling studies, *J. Instrum.* 6 (2011) P04006.
- [11] P. Schoofs, Monte carlo modeling of crystal channeling at high energies (Ph.D. thesis), Ecole Polytechnique Federale de Lausanne, 2014.